EFEMP1-Mediated Regulation of Choroidal Vascular Dysfunction in Myopia: Insights Into the FOXO3/VEGFA Pathway as a Therapeutic Target

Wen-Qing Shi,[1] Bing Li,[1] Yuting Shao,[1] Wenting Han,[1] Yule Xu,[1] Qing Jiang,[1] Shen Qu,[1] Xiaodong Zhou,[2] and Yanlong Bi[1]

[1]Department of Ophthalmology, Tongji Eye Institute, Tongji Hospital, School of Medicine, Tongji University, Shanghai, People's Republic of China
[2]Department of Ophthalmology, Jinshan Hospital, Fudan University, Shanghai, People's Republic of China

Correspondence: Xiaodong Zhou, Department of Ophthalmology, Jinshan Hospital, Fudan University, Shanghai 201518, People's Republic of China; xdzhou_2013@163.com.
Yanlong Bi, Department of Ophthalmology, Tongji Eye Institute, Tongji Hospital, School of Medicine, Tongji University, Shanghai 200065, People's Republic of China; biyanlong@tongji.edu.cn.

Received: October 31, 2024
Accepted: February 27, 2025
Published: March 20, 2025

Citation: Shi WQ, Li B, Shao Y, et al. EFEMP1-mediated regulation of choroidal vascular dysfunction in myopia: Insights into the FOXO3/VEGFA pathway as a therapeutic target. *Invest Ophthalmol Vis Sci.* 2025;66(3):43. https://doi.org/10.1167/iovs.66.3.43

Purpose. This study investigates the role of EFEMP1 in choroidal vascular dysfunction and its implications for myopia progression, specifically focusing on the FOXO3/VEGFA signaling pathway as a potential therapeutic target.

Methods. We utilized adeno-associated virus (AAV) to overexpress and knock down EFEMP1 in the choroid of guinea pigs. Subsequent proteomic analyses were conducted on the choroidal tissue. We used Gene Ontology (GO) and the Kyoto Encyclopedia of Genes and Genomes (KEGG) to identify relevant pathways and genes. In vitro experiments were performed on RF/6A cells, where both EFEMP1 and FOXO3 underwent overexpression and knockdown. We conducted a series of cell culture experiments, including assessments of cell proliferation, migration, tube formation, and choroidal sprouting assays, to evaluate the functional effects of EFEMP1. Quantitative reverse transcription PCR and Western blot analyses were utilized to measure gene and protein expression levels.

Results. Silencing EFEMP1 significantly reduced choroidal vascular dysfunction and slowed the progression of myopia. Proteomic analysis demonstrated that EFEMP1 regulates FOXO3 activity, resulting in increased VEGFA expression in RF/6A cells and promoting angiogenesis. Conversely, knockdown of FOXO3 led to decreased VEGFA levels, confirming that EFEMP1 modulates VEGFA expression through FOXO3.

Conclusions. Targeting EFEMP1 may offer a novel therapeutic strategy for the prevention and treatment of myopia by alleviating associated vascular dysregulation. Further exploration of the FOXO3/VEGFA pathway could provide additional insights into therapeutic interventions for myopia.

Keywords: myopia, choroid, sclera, VEGFA, EFEMP1

Globally, the high prevalence and rapid increase of myopia have become urgent issues in public health, particularly among adolescents.[1] The early onset and rapid progression of myopia not only affect quality of life but may also lead to a range of serious complications, such as retinal detachment and macular degeneration.[2] Therefore, in-depth research into the pathogenesis of myopia is essential for elucidating its pathological processes and identifying effective interventions.

Choroidal vascular dysfunction has increasingly been recognized as a significant factor in the pathogenesis of myopia.[3] The choroid is a crucial structure that supplies oxygen and nutrients to the retina; abnormalities in its vascular function may lead to metabolic imbalances within the choroid itself, which subsequently triggers scleral remodeling. Scleral remodeling is the central pathological process underlying the progression of myopia, and choroidal vascular dysfunction may accelerate the development of myopia by altering the composition and structure of the scleral extracellular matrix.[4] Therefore, choroidal vascular dysfunction plays a pivotal role in the pathogenesis of myopia and may serve as a critical target for research aimed at myopia prevention and treatment.

Our previous studies have identified EGF-containing fibulin-like extracellular matrix protein 1 (EFEMP1) as a key regulatory factor in the remodeling of the scleral extracellular matrix.[5] We found that EFEMP1 expression is significantly increased in the tears of myopic individuals and in the choroids of form-deprivation myopic (FDM) guinea pigs, suggesting that EFEMP1 may be implicated in the onset and progression of myopia.[6] More importantly, the intricate relationship between choroidal vascular dysfunction and scleral remodeling implies that EFEMP1 may play a dual role in regulating these processes.

Based on this background, the present study further explores the mechanisms by which EFEMP1 influences choroidal vascular dysfunction associated with myopia through in vivo and in vitro experiments. The experimental results indicate that silencing EFEMP1 expression effectively inhibits choroidal vascular dysfunction and signifi-

cantly delays the progression of myopia. Thus, modulating EFEMP1 levels to intervene in choroidal vascular dysfunction may represent a novel strategy for the prevention and treatment of myopia.

Methods

Animals

All animal experiments comply with the relevant statements from the Association for Research in Vision and Ophthalmology (ARVO) regarding the use of animals in ophthalmic and vision research. The experimental subjects consisted of male British Shorthair guinea pigs, aged 2 weeks, with a body weight ranging from 100 to 150 grams. The animals were housed in a temperature-controlled environment with a 12-hour light/12-hour dark photoperiod, ensuring they had daily access to adequate food and water. Additionally, fresh vegetables were included in their diet to enhance nutritional intake and diversify their feeding regimen.

Induction of FDM and Biological Parameter Measurement

The guinea pigs were divided into a control group and an FDM group randomly. The control group received no treatment, whereas the FDM group had their right eye covered with a homemade hood (made from latex balloons), ensuring that other parts were normally exposed to prevent interference with feeding and activity.

The eyes of the guinea pigs were pretreated with compounded tobramycin eye drops, administered 3 times with intervals of approximately 5 minutes. The tested guinea pigs were then moved to a dark room, where the examiner uses a streak retinoscope (Six-Six Vision Technology, China) for retinoscopy. The retinoscope was positioned about 50 cm from the guinea pig, and the calculation formula for equivalent spherical lenses was the spherical degree plus half the cylindrical degree minus 2.0 diopters (D), repeated 3 times and recorded to an accuracy of 0.01 D. All guinea pigs had an interocular refractive difference of <3.00 D. The axial length of the guinea pig was measured using an A ultrasound probe (Kaixin Electronic Instrument, China), with 10 measurements taken to obtain an average, precision to 0.01 mm, enabling the determination of the final axial length.

AAV Vector Construction and Intravitreal Injection

The pcAAV-CMV-EFEMP1-3 × FLAG-P2A-GdGreen-WPRE plasmid vector (Supplementary Fig. S1) was co-transfected with pHelper, which contains adenoviral genes, and pAAV-RC, which includes AAV replication and coat genes, into AAV-293 cells. The resulting virus was designated as AAV-EFEMP1. Additionally, shRNA and corresponding empty viral vectors were packaged and amplified, marked as AAV-shEFEMP1, AAV-NC, and AAV-Vector, respectively (the sequence is shown in Supplementary Table S1). Three days after transfection, the recombinant AAV complete assembly in the packaging cells.[7] The virus was then harvested and purified, with a final titer of approximately 10^{12} to 0^{13} copies per milliliter.[8]

After anesthetizing the guinea pigs with isoflurane, 2 µL of AAV was injected intravitreally into the right eye of each guinea pig in the treated groups (n = 10 in each group) using a Hamilton microinjector (Sigma-Aldrich, USA) under a microscope. After injection, the needle was slowly withdrawn after a 2-second pause, and an eye gel containing levofloxacin hydrochloride was applied to prevent infection.

Enzyme-Linked Immunosorbent Assays

Guinea pigs were euthanized via intraperitoneal injection of 1% pentobarbital sodium, and then 2 mL of blood was collected from each group of guinea pigs. After centrifugation, the serum samples were quantitatively analyzed for EFEMP1 content using an enzyme-linked immunosorbent assay (ELISA) kit (Enzyme-linked Biotechnology Co., Ltd., Shanghai, China). Each well received 50 µL of standard, sample, and biotin-labeled antibody, followed by incubation at room temperature for 1 hour, and then washed for 5 minutes, and repeated 3 times. Subsequently, 80 µL of HRP-conjugated label was added, followed by incubation at room temperature for 30 minutes, and again washed for 5 minutes, and repeated 3 times, before adding the enzyme substrate. After washing, the microplate was quickly scanned, and 50 µL of stop solution was added. Finally, the optical density (OD) value was measured at 450 nm using an ELISA reader (Thermo Fisher Scientific, USA) to quantify the EFEMP1 concentration in the serum samples.

Proteomic Analysis

After protein extraction, purification, and trypsin digestion of the choroidal tissue samples from each group, the proteins were reduced and alkylated, followed by analysis using liquid chromatography-mass spectrometry (LC-MS). The chromatography system's preset 100 samples per day (SPD) method was used for peptide separation.[9] After ionization using a capillary ion source, data were acquired using the timsTOF Pro 2 mass spectrometer in the dia-PASEF acquisition mode.[10] Differential expression proteins (DEPs) were identified through t-tests (P value < 0.05) and fold changes greater than 1.5 or less than 0.5.

Cell Culture and Transfection

RF/6A cells (FuHeng Cell Center, Shanghai, China) were cultured in DMEM medium supplemented with 10% fetal bovine serum (FBS; Thermo Fisher Scientific) and incubated in a humidified incubator at 37°C with 5% carbon dioxide. The siRNA and plasmid targeting EFEMP1 and FOXO3 were synthesized by GenePharma (Shanghai, China; the sequence is shown in Supplementary Table S4). All transfections were performed using Lipofectamine 3000 (Thermo Fisher Scientific) according to the manufacturer's instructions.

Cell Proliferation Assay

When the cells reached approximately 70% to 80% confluence, 20 µM EdU working solution and an equal volume of medium were added for a 2-hour incubation. Cells were washed with PBS and fixed with 4% paraformaldehyde. After permeabilization with a permeabilization solution (0.3% Triton X-100 in PBS), an appropriate amount of Click reaction solution was added to visualize the EdU-labeled cells. Finally, EdU-positive cells were observed and counted using a fluorescence microscope to assess cell proliferation.

Investigative Ophthalmology & Visual Science

Cell Migration Assay

A Transwell chamber with 8.0 mm pores (Corning Life Sciences, Corning, NY, USA) was placed in a 24-well plate, and RF/6A cells were seeded at a density of 1×10^4 cells in the upper chamber, whereas DMEM with 10% FBS was added to the lower chamber. After 24 hours, the cells are fixed with 4% paraformaldehyde, and non-migrated cells on the upper surface were removed. The migrated cells were subsequently stained with crystal violet and counted using an inverted microscope (Olympus, Tokyo, Japan).

Tube Formation Assay

Matrigel was added to the culture plate and solidified at 37°C. Then, the cells to be tested were seeded onto the solidified Matrigel surface and nurtured for 6 hours to promote cell growth and tubular structure formation. The structure and number of tubes were observed under a microscope (Olympus, Tokyo, Japan), and the total length of tubes and branch points were measured using ImageJ software or other image analysis tools to quantify the tube formation ability of the cells.

Quantitative Reverse Transcription PCR

Total RNA was extracted from RF/6A cells or choroidal tissues using the RNA-Quick Purification Kit (ES Science, Shanghai, China). The extracted RNA was then converted to complementary DNA (cDNA) through reverse transcription using the PrimeScript RT Master Mix (Takara, Shiga, Japan). Specific primers targeting the genes of interest were designed (see Supplementary Table S2). Amplification reactions were performed using a real-time fluorescence quantitative PCR instrument, with SYBR Green probes used for fluorescence monitoring. The fluorescence intensity of the PCR amplification was recorded in real time. Relative expression levels of the target genes were calculated by comparing the cycle threshold (Ct) values of the target genes to those of GAPDH, utilizing the $2^{-\Delta\Delta Ct}$ method for data analysis. Each sample was tested in triplicate to ensure the accuracy and reproducibility of the results.

Western Blot

Following the collection of the cell or choroidal tissue samples, protein extraction was performed using a lysis buffer (Beyotime Biotechnology, China). After centrifugation, the supernatant was obtained to remove cell debris. The protein concentration was determined using the BCA method (Beyotime Biotechnology, China), and equal amounts of protein samples were separated using SDS-PAGE. After electrophoresis, proteins were transferred to a polyvinylidene difluoride (PVDF) membrane and treated with blocking solution (5% skim milk) to reduce nonspecific binding. Primary antibodies (see Supplementary Table S3) and corresponding HRP-conjugated secondary antibodies were sequentially added to the membrane, followed by washing, and color development was performed using a chemiluminescent substrate (ECL; Merck Millipore, Germany). Finally, the results were recorded and quantitatively analyzed using an imaging system.

Choroid Sprouting Assay

The choroid-retinal pigment epithelium (RPE)-sclera complex was cut into thin slices approximately 2 mm × 1 mm and placed in a 24-well plate coated with Matrigel (BD Biosciences, Cat. 354230). After the choroid was plated, it was incubated without medium for 10 minutes in a 37°C incubator to allow the Matrigel to solidify. Subsequently, 500 µL of medium was added to each well, and the plates were incubated at 37°C and 5% CO2 for 48 hours before any treatments were applied. The medium was replaced every 48 hours, and observations were made at days 1, 4, and 7 using a microscope (Nikon, Tokyo, Japan).

Immunohistochemistry

After preparing the sections from tissue samples, the sections were washed with PBS and subjected to deparaffinization and rehydration. Antigen retrieval methods were used to enhance the accessibility of antibody binding sites. The treated sections were then processed with blocking solution to reduce background noise. Specific primary antibodies were added to the sections, followed by incubation overnight at 4°C to enhance binding efficiency. After incubation, PBS washing was conducted, and HRP or fluorescently labeled secondary antibodies are added, followed by additional washing. Finally, color development was performed using DAB or fluorescent dyes, and the results were recorded and observed under a microscope (BH-2, Olympus, Japan).

Statistical Analysis

We leveraged the R software package to conduct Kyoto Encyclopedia of Genes and Genomes (KEGG) pathway enrichment analysis with the intent of explicating functional enrichment and constructing clusters, as well as to delineate the diversity among genes/proteins with differential functions. For statistical analyses and graphic representations, SPSS version 25.0, GraphPad Prism 9 and R version 3.5.2 were utilized. Differences between groups were assessed using Chi-square tests, Student's *t*-tests, Mann-Whitney *U* tests, and Friedman tests. For experimental components involving comparisons across multiple groups, 1-way analysis of variance (ANOVA) was used, followed by Bonferroni post hoc tests for multiple comparisons. The *t*-tests were administered for analyses involving only two groups. All outcomes are presented as mean ± standard error of the mean (mean ± SEM). A *P* value of less than 0.05 was considered the threshold for statistical significance in this study.

Results

Increased Expression of EFEMP1 in the Blood of FDM Guinea Pigs

To explore the changes in EFEMP1 expression in the blood of FDM guinea pigs, we collected serum samples from guinea pigs that had their right eyes covered for 4 weeks, as well as from control group guinea pigs. Compared to the control group, the FDM group exhibited a significant myopic shift characterized by decreased refraction and a marked increase in axial length (Figs. 1A, 1B). Moreover, the EFEMP1 content in the serum of FDM guinea pigs was significantly higher than that in the control group (Fig. 1C).

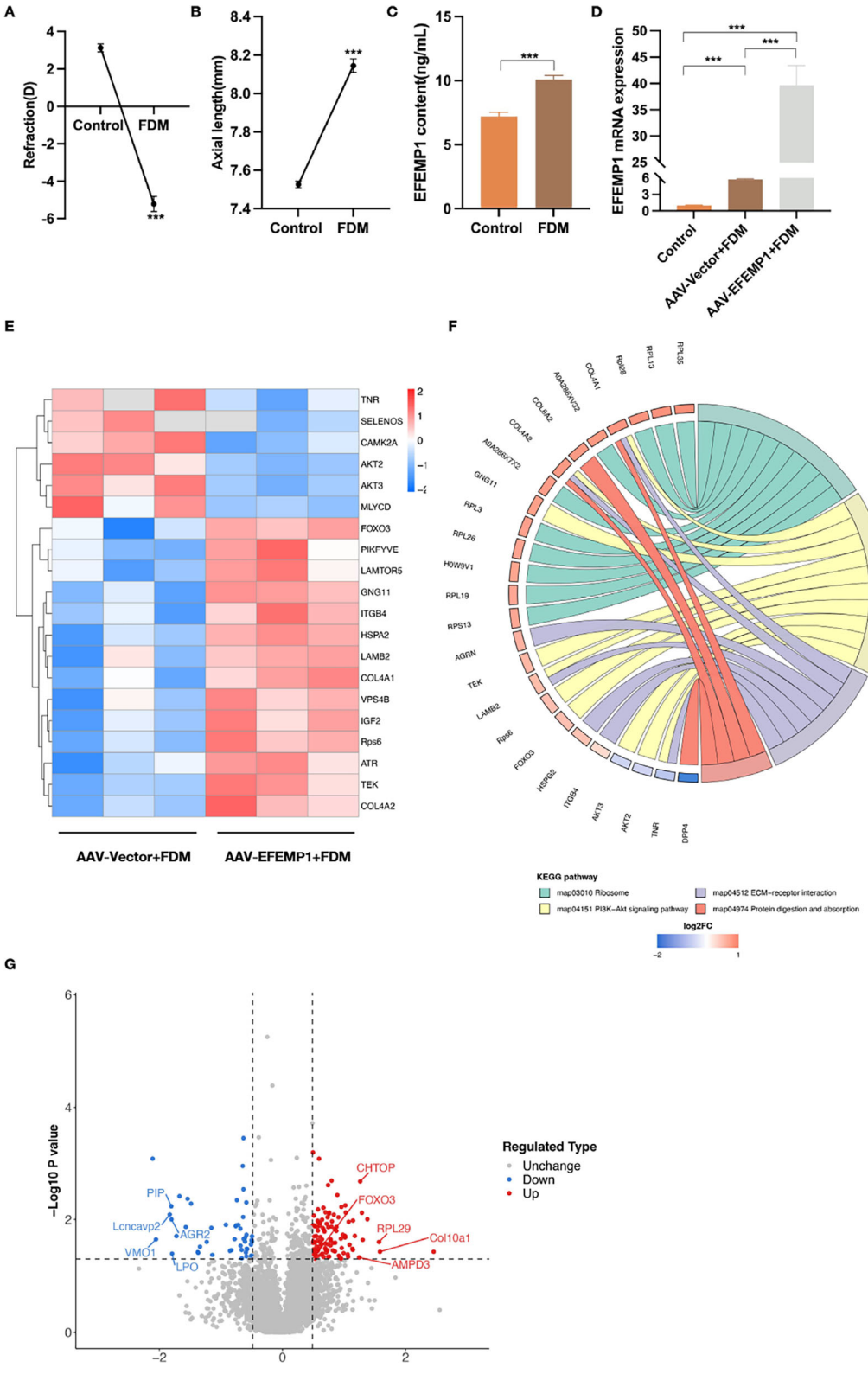

Figure 1. Expression of EFEMP1 in guinea pig serum and the impact of its overexpression on the cytokine expression profile. (**A, B**) Comparison of the right eye refraction **A** and axial length **B** of different groups of guinea pigs after 4 weeks of form-deprivation treatment ($n = 10$ in each group, $^{***}P < 0.001$, Mann-Whitney U test, and Bonferroni test). (**C**) Comparison of EFEMP1 contents in the serum of two groups of guinea pigs ($n = 10$ in each group, $^{***}P < 0.001$, unpaired two-tailed t-tests). (**D**) The effect of AAV-mediated overexpression of EFEMP1 on EFEMP1 mRNA expression ($^{***}P < 0.001$, 1-way ANOVA, and Bonferroni test). (**E**) Heatmap representation of differentially expressed genes regulated by overexpression of EFEMP1. (**F**) Identification of proteins enriched in functional pathways through KEGG analysis. (**G**) Scatter plot representation of differentially expressed genes regulated by overexpression of EFEMP1 (panels **E** and **F** were created using R version 3.5.2 and ggplot2 version 3.3.5).

Investigative Ophthalmology & Visual Science

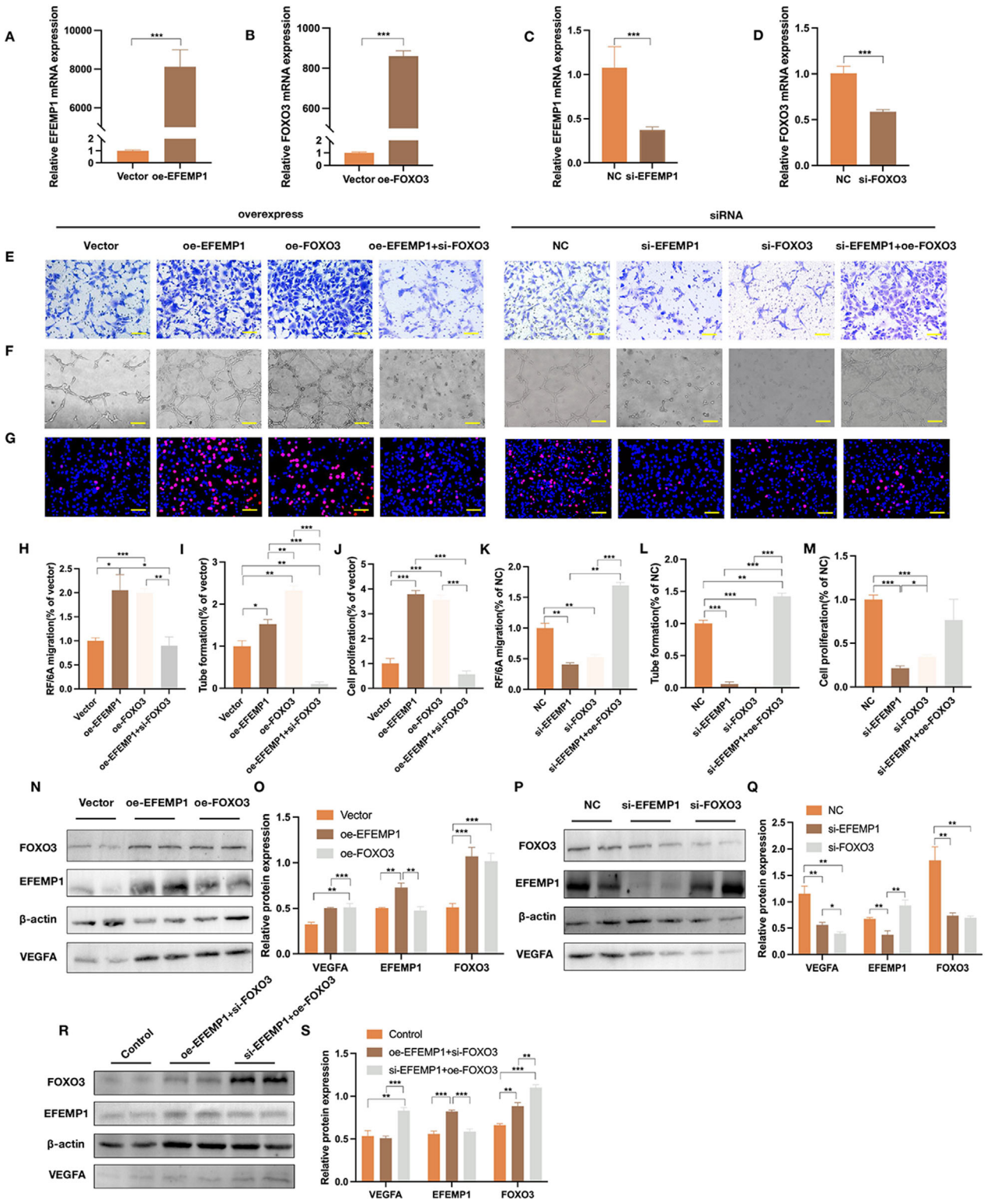

Figure 2. Overexpression or knockdown of EFEMP1 promotes or inhibits the invasion, tube formation, and proliferation of RF/6A cells through the FOXO3/VEGFA pathway. (**A, B**) The mRNA expression levels of EFEMP1 **A** and FOXO3 **B** after transfecting RF/6A cells with the pcDNA 3.1 vector, pcDNA 3.1-EFEMP1 (oe-EFEMP1), and pcDNA 3.1-FOXO3 (oe-FOXO3; ***$P < 0.001$ unpaired two-tailed *t*-tests, $n = 6$); (**C, D**) The mRNA expression levels of EFEMP1 **C** and FOXO3 **D** after interfering with RF/6A cells using siRNA-EFEMP1 (si-EFEMP1) and siRNA-FOXO3 (si-FOXO3; ***$P < 0.001$ unpaired two-tailed *t*-tests, $n = 6$). (**E–M**) The effects of EFEMP1 overexpression (OE-EFEMP1), FOXO3 overexpression (oe-FOXO3), and simultaneous knockdown of FOXO3, whereas overexpressing EFEMP1 (oe-EFEMP1 + si-FOXO3), si-EFEMP1, and si-FOXO3, and the simultaneous knockdown of EFEMP1 whereas overexpressing FOXO3 (si-EFEMP1 + oe-FOXO3) on the invasion (**E, H, K**), tube formation (**F, I, L**), and proliferation (**G, J, M**) of RF/6A cells (*$P < 0.05$, **$P < 0.01$; and ***$P < 0.001$; 1-way ANOVA, Bonferroni test; Bar = 100 µm, $n = 6$). (**N–O**) The effects of overexpressing EFEMP1 and FOXO3 in RF/6A on the expression of

EFEMP1/FOXO3/VEGFA pathway proteins (*$P < 0.05$, **$P < 0.01$, and ***$P < 0.001$, 1-way ANOVA, and Bonferroni test, $n = 6$). (**P–Q**) The impact of knocking down EFEMP1 and FOXO3 in RF/6A on the expression of EFEMP1/FOXO3/VEGFA pathway proteins (*$P < 0.05$, **$P < 0.01$, and ***$P < 0.001$, 1-way ANOVA, and Bonferroni test, $n = 6$). (**R, S**) The effects of oe-EFEMP1 + si-FOXO3 and si-EFEMP1 + oe-FOXO3 on the expression of EFEMP1/FOXO3/VEGFA pathway proteins (*$P < 0.05$, **$P < 0.01$, and ***$P < 0.001$, 1-way ANOVA, and Bonferroni test, $n = 6$).

Protein Expression Related to EFEMP1 Overexpression in the Choroid

To identify the molecular mechanisms associated with the pathogenesis of myopia in the choroid following EFEMP1 overexpression, we performed intravitreal injections using AAV. The results showed that EFEMP1 was significantly elevated in the choroid of the AAV-EFEMP1 + FDM group compared to the control group (Fig. 1D). Subsequently, proteomic analysis of the choroidal tissue from the FDM model was performed. Initially, the fold change (log2 |fold change| > 1) was set as the criterion for differentially expressed genes (DEGs). Compared to the AAV-Vector + FDM group, 261 DEGs were identified in the AAV-EFEMP1 + FDM group, including 181 DEGs such as FOXO3, that were upregulated, whereas the remaining 80 were downregulated. KEGG analysis indicated that DEGs were highly enriched in signaling pathways such as ribosome, ECM-receptor interaction, and PI3K-AKT (Figs. 1E, 1F, 1G).

Regulatory Roles of EFEMP1 and FOXO3 in Choroidal Cell Functions

To determine the role of EFEMP1 in RF/6A cells in vitro, we transfected RF/6A cells with siRNA and overexpression plasmids for EFEMP1 and FOXO3. Overexpression of EFEMP1 (oe-EFEMP1) and FOXO3 (oe-FOXO3) resulted in increased expression in RF/6A cells compared to the Vector group (Figs. 2A, 2B). In contrast to the negative control (NC) group, silencing of EFEMP1 (si-EFEMP1) and FOXO3 (si-FOXO3) led to decreased expression of EFEMP1 and FOXO3 in RF/6A cells (Figs. 2C, 2D). Transwell and Matrigel tube formation assays demonstrated that overexpression of EFEMP1 and FOXO3 significantly enhanced the migratory and tube-forming abilities of RF/6A cells (Figs. 2E, 2F, 2H, 2I). Conversely, silencing of EFEMP1 and FOXO3 inhibited the migratory and tube-forming abilities of RF/6A cells (Figs. 2E, 2F, 2K, 2L). EdU (5-ethynyl-2′-deoxyuridine) assays showed that both EFEMP1 and FOXO3 overexpression significantly increased the proliferation of RF/6A cells (Figs. 2G, 2J). Conversely, silencing EFEMP1 and FOXO3 inhibited the proliferative capacity of RF/6A cells (Figs. 2G, 2M).

EFEMP1 Regulates Choroidal Vascular Function Via FOXO3/VEGFA

The overexpression of EFEMP1 led to increased expression levels of EFEMP1, FOXO3, and VEGFA in RF/6A cells, whereas overexpression of FOXO3 alone also significantly upregulated VEGFA expression (Figs. 2N, 2O). In contrast, when siRNA was used to inhibit EFEMP1 and FOXO3 expressions in RF/6A, both FOXO3 and VEGFA levels significantly decreased (Figs. 2P, 2Q). To further verify whether EFEMP1 regulates choroidal cell function and VEGFA through FOXO3, we applied si-FOXO3 to RF/6A after overexpressing EFEMP1 and found that cell proliferation, migration, and tube formation were inhibited (Figs. 2E–M), whereas VEGFA expression decreased (Figs. 2R–S). Additionally, following the knockdown of EFEMP1 with oe-FOXO3, we observed significant increases in the migration and tube formation abilities of cells compared to the groups with only si-EFEMP1 or si-FOXO3 (Figs. 2E–M), and VEGFA protein levels were also significantly elevated (Figs. 2R–S).

AAV-EFEMP1 Intravitreal Injection Induces Myopic Shift and Aggravates Ex Vivo Choroidal Vascular Dysfunction in Guinea Pigs

Based on the evidence outlined above, we established the key role of EFEMP1 in choroidal cells and investigated whether EFEMP1 is implicated in the pathogenesis of myopia. We utilized AAV to deliver the overexpressed EFEMP1 plasmid via intravitreal injection into FDM guinea pigs 1 week after modeling to elevate EFEMP1 levels in the choroid. The results showed that the AAV-EFEMP1 + FDM group exhibited significantly increased levels compared to the AAV-Vector + FDM and control groups (see Fig. 1D). After 3 weeks of injections, the degree of myopia in the AAV-EFEMP1 + FDM group significantly increased compared to the AAV-Vector + FDM group, with axial length changes that were more increased (Figs. 3A–D). We used a choroidal sprouting model to evaluate the effects of EFEMP1 overexpression in the choroid. The results indicated that EFEMP1 overexpression significantly enhanced the angiogenic activity of the choroid ex vivo (Figs. 3E, 3F). Western blot analysis revealed that after 4 weeks of FDM treatment, the expressions of EFEMP1, FOXO3, and VEGFA in the choroid of guinea pigs were significantly increased (Figs. 3G, 3H). Immunohistochemistry results further showed that the expression of the fibroblast marker COL1A1 in the sclera was reduced, whereas the expression of the myofibroblast marker α-SMA was increased (Fig. 3I).

Inhibiting EFEMP1 Delays the Progression of Myopia and Suppresses Choroidal Vascular Dysfunction Ex Vivo

We designed shRNA to reduce the levels of EFEMP1 in the choroid of guinea pigs (Fig. 4A). Likewise, intravitreal injections were applied to guinea pigs 1 week after FDM treatment. After 4 weeks of FDM treatment, the silencing of EFEMP1 led to significant improvement in refractive error when compared to the AAV-NC + FDM group (Figs. 4B, 4D), whereas simultaneously delaying the extension of axial length (Figs. 4C, 4E). Ex vivo sprouting experiments demonstrated that inhibiting EFEMP1 could significantly diminish the sprouting ability of choroidal endothelial cells (Figs. 4F, 4G). Additionally, expression levels of EFEMP1, FOXO3, and VEGFA in the choroid of guinea pigs were significantly suppressed (Figs. 4H, 4I), whereas the expression of COL1A1 in the sclera increased significantly and α-SMA expression decreased (Fig. 4J).

Investigative Ophthalmology & Visual Science

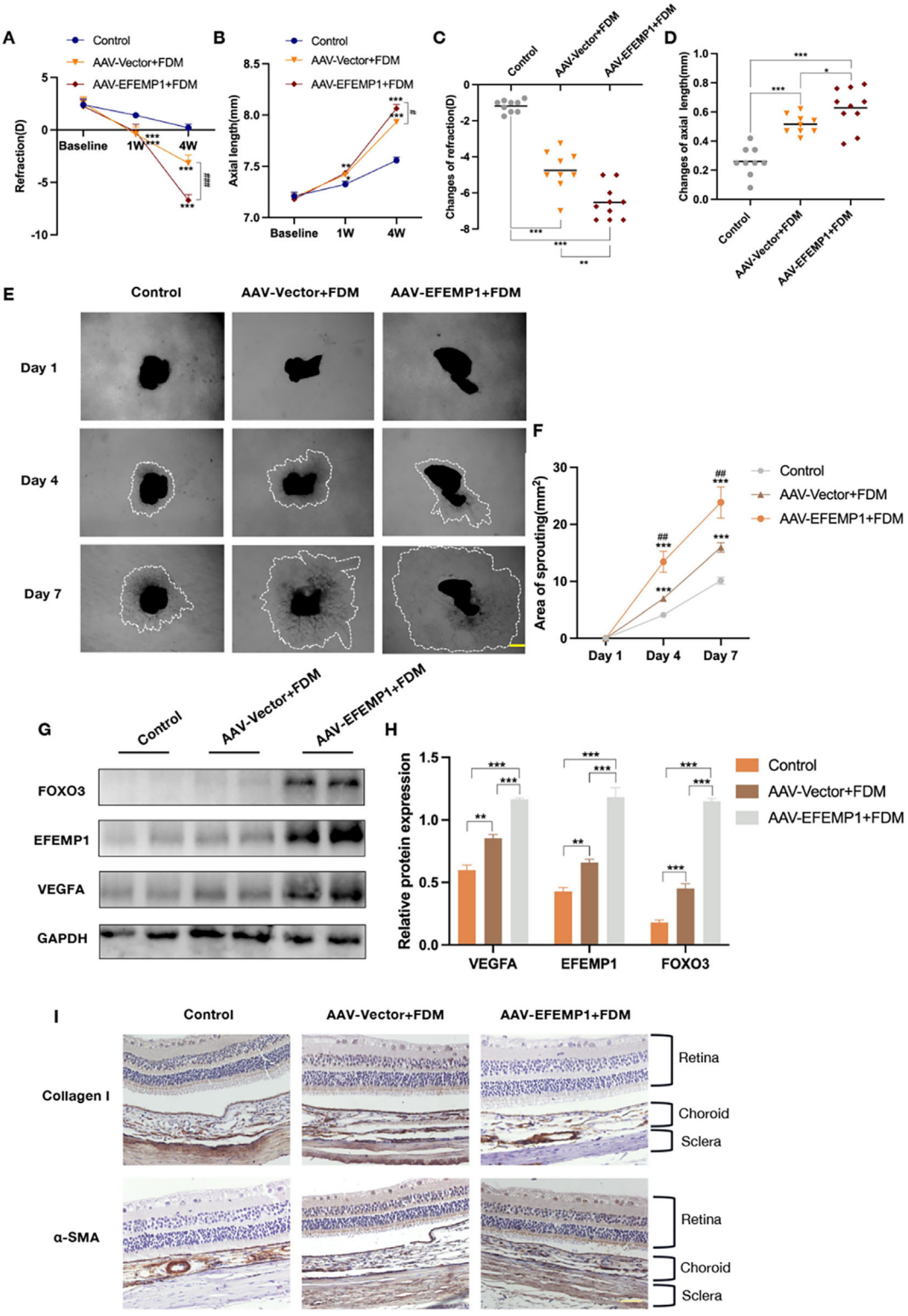

Figure 3. EFEMP1 overexpression promotes myopia in FDM guinea pigs and regulates choroidal vascular function in vivo and ex vivo. (**A–D**) Changes in biological parameters of the right eye of each group of guinea pigs before and after the intravitreal injection of AAV-EFEMP1 (*P < 0.05, **P < 0.01, and ***P < 0.001, versus the control group, $^{\#\#}P$ <0.01 and $^{\#\#\#}P$ <0.001, versus AAV-Vector + FDM group, 2-way repeated measures ANOVA, and Bonferroni tests, $n = 6$ of each group). (**E, F**) Choroidal sprouting assay results for each group on days 1, 4, and 7 (Bar = 500 µm, *P < 0.05, **P < 0.01, and ***P < 0.001, versus the control group, $^{\#\#}P$ < 0.01 and $^{\#\#\#}P$ < 0.001, versus the AAV-Vector + FDM group, Mann-Whitney U test, and Bonferroni test, $n = 5$). (**G, H**) The expression of EFEMP1/FOXO3/VEGFA pathway proteins after intravitreal injection (*P < 0.05, **P < 0.01, and ***P < 0.001, 1-way ANOVA, and Bonferroni tests, $n = 6$). (**I**) Representative immunohistochemical staining images of Collagen I and α-SMA in the sclera of each group (Bar = 50 µm).

Investigative Ophthalmology & Visual Science

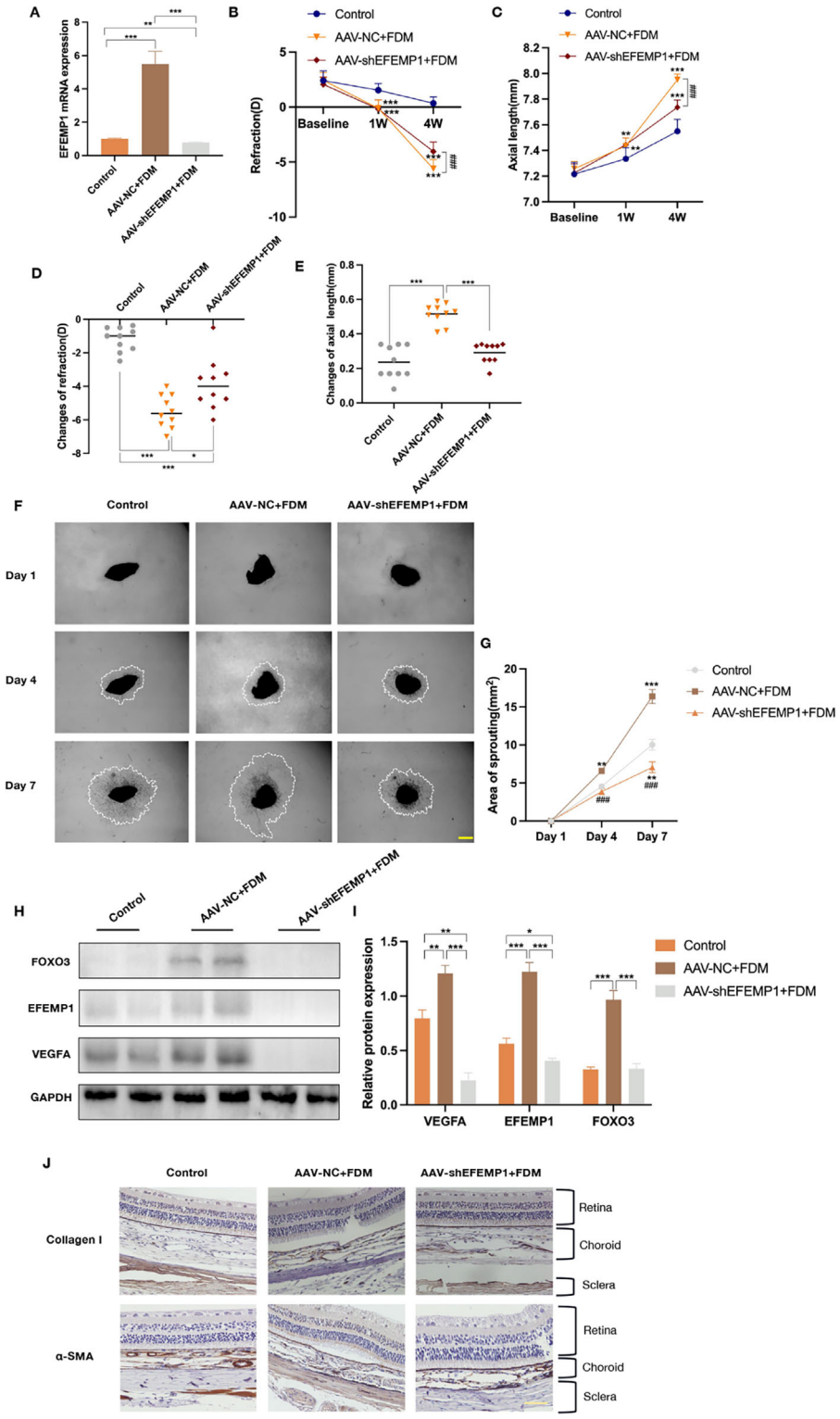

Figure 4. Knockdown of EFEMP1 retards the progression of myopia in FDM guinea pigs and inhibits choroidal vascular function in vivo and ex vivo. (**A**) The expression levels of EFEMP1 mRNA in the choroid of each group after injection of AAV-shEFEMP1 (**$P < 0.01$ and ***$P < 0.001$, two-way ANOVA, and Bonferroni test, $n = 10$ in each group). (**B–E**) Changes in biological parameters of the right eye of each group of FDM guinea pigs before and after injection of AAV-EFEMP1 **B** and **C** (*$P < 0.05$, **$P < 0.01$, and ***$P < 0.001$, versus the control group, $^{\#\#}P < 0.01$ and $^{\#\#\#}P < 0.001$, versus the AAV-NC + FDM group, two-way repeated measures ANOVA, and Bonferroni tests; **D** and **E**, *$P < 0.05$, **$P < 0.01$, and ***$P < 0.001$, two-way ANOVA, and Bonferroni test, $n = 10$ in each group). (**F, G**) Results of the choroidal sprouting assay for each group on days 1, 4, and 7 (Bar = 500 µm, *$P < 0.05$, **$P < 0.01$, and ***$P < 0.001$, versus the control group, $^{\#\#}P < 0.01$ and $^{\#\#\#}P < 0.001$, versus the AAV-NC + FDM group, Mann-Whitney U test, and Bonferroni test, $n = 5$). (**H, I**) The expression of the EFEMP1/FOXO3/VEGFA pathway proteins after intravitreal injection of AAV-shEFEMP1 (*$P < 0.05$, **P <0.01, and ***$P < 0.001$, one-way ANOVA, and Bonferroni tests, $n = 6$). (**J**) Representative immunohistochemical staining images of Collagen I and α-SMA in the sclera of each group (Bar = 50 µm).

Investigative Ophthalmology & Visual Science

Discussion

Our preliminary study suggests that EFEMP1 influences the onset and progression of myopia by modulating the composition and structural integrity of the extracellular matrix.[5] The role of the extracellular matrix within the sclera is crucial for maintaining ocular structure, with remodeling critical to axial elongation and myopia development.[11] Hence, the function of EFEMP1 in myopia progression warrants further investigation to elucidate its role in myopia pathogenesis of this condition.

Current research highlights the pivotal role of reduced choroidal blood flow-induced scleral hypoxia in the development of myopia.[12,13] Such hypoxia not only hastens myopia progression but might also foster atypical extracellular matrix remodeling by activating particular signaling paths.[14,15] This mechanism represents an expanding area of focus in the pathophysiological study of myopia. Previously, we observed anomalously elevated expression of EFEMP1 in the choroid of FDM guinea pigs, indicating its potential significance in choroidal pathology.[6] This study utilized AAV vectors to overexpress EFEMP1 in the choroids of guinea pigs and subsequently investigated related signaling pathways and molecular mechanisms through proteomic sequencing.

The proteomic analysis in this study demonstrated that EFEMP1 overexpression resulted in aberrant expression of molecules primarily involved in the ribosome and PI3K/AKT pathways. These findings underscore EFEMP1's potential to modulate cellular function and disease progression, prompting a more in-depth exploration of its mechanistic impact on myopia and choroidal angiogenesis. In studies of other ocular diseases, such as Leventinese disease and Doyne honeycomb retinal dystrophy, it has been established that the abnormal expression of EFEMP1 can activate the unfolded protein response and increase VEGF expression.[16] Furthermore, EFEMP1 significantly influences angiogenesis in conditions such as primary hypertension by regulating the expression of vascular endothelial growth factor A (VEGFA).[17]

The transcription factor Recombinant Forkhead Box Protein O3 (FOXO3), regulated by EFEMP1, has garnered interest due to its involvement in autophagy, apoptosis, and oxidative stress, as well as its potential modulation of angiogenesis through the regulation of VEGFA transcription. This provides valuable insights for further exploration into molecular mechanisms.[18–23] Research has demonstrated FOXO3's capability to suppress VEGFA expression via the miRNA pathway, thereby inhibiting angiogenesis and tumor metastasis.[24] In rheumatoid arthritis, the FOXO3/VEGFA pathway appears to govern angiogenic activities, aligning with our study's findings and suggesting FOXO3's broader regulatory influence on angiogenesis across various pathological situations.[25] Additionally, VEGFA expression is significantly elevated under hypoxic conditions, with the hypoxia-inducible factor (HIF) serving as a crucial transcriptional activator that enhances VEGFA transcription, promoting vascular endothelial cell proliferation and angiogenesis.[26–29] As myopia progresses, the vascular structure and hemodynamics of the choroid are altered, resulting in hypoxia and inflammatory responses in the ocular tissues. This environment promotes VEGFA expression and exacerbates choroidal neovascularization associated with myopia.[30–32]

In the context of our myopic model, FOXO3's regulation of VEGFA expression levels appeared to influence choroidal angiogenesis. To delineate the interplay among EFEMP1, FOXO3, and VEGFA, we conducted a suite of in vitro experiments using RF/6A cells, manipulating EFEMP1 and FOXO3 expression through plasmid-mediated overexpression and siRNA-induced knockdown. Our findings indicated that overexpression of EFEMP1 significantly enhanced FOXO3 activity, which in turn elevated VEGFA expression. Conversely, FOXO3 knockdown substantially reduced VEGFA levels, suggesting that EFEMP1 may indirectly regulate VEGFA through FOXO3, thus impacting choroidal vessel formation. This novel regulatory mechanism offers an innovative perspective on the pathogenesis of myopia. Subsequent in vivo assays confirmed these findings, revealing that overexpression of EFEMP1 in the choroidal tissue of FDM guinea pigs significantly accelerated the progression of myopia. Utilizing the choroid sprouting assay, we observed a marked increase in the vascularization potential of the choroidal tissue in FDM guinea pigs with EFEMP1 overexpression. Furthermore, we noted a concurrent reduction in COL1A1 levels and an increase in α-SMA levels within the sclera, which aligns with alterations in choroidal angiogenesis. These results suggest that EFEMP1 may regulate angiogenesis through the FOXO3/VEGFA axis and contribute to scleral remodeling.

In summary, our study evidences that EFEMP1 orchestrates choroidal angiogenesis through the FOXO3/VEGFA pathway, potentially precipitating significant scleral structural alterations amid myopia pathology. These insights reinforce the notion that future investigations should explore the dual regulatory effects of EFEMP1 on both choroidal and scleral pathology while assessing its therapeutic potential as a target. Moreover, subsequent research should investigate HIF's regulatory role on the FOXO3/VEGFA axis under hypoxic conditions, as well as the effects of blocking VEGF on the expression of EFEMP1 and FOXO3, to gain a deeper understanding of the role of this pathway in pathological angiogenesis.

Acknowledgments

Supported by the National Natural Science Foundation of China (82070920), Key cultivation disciplines of Shanghai Tongji Hospital (ZDPY24-YK), Shanghai Municipal Health Commission Clinical Research Special Projects (202340282).

Author Contributions: All listed authors have contributed to the manuscript substantially and have agreed to the final submitted version.

Availability of Data and Materials: The datasets used and/or analyzed during the present study are available from the corresponding author on reasonable request.

Ethical Approval and Consent to Participate: The study methods and protocols were approved by the Medical Ethics Committee of the Shanghai Tongji Hospital and followed the principles of the Declaration of Helsinki. All subjects were notified of the objectives and content of the study and latent risks, and then provided written informed consent to participate.

Disclosure: **W.-Q. Shi**, None; **B. Li**, None; **Y. Shao**, None; **W. Han**, None; **Y. Xu**, None; **Q. Jiang**, None; **S. Qu**, None; **X. Zhou**, None; **Y. Bi**, None

References

1. Baird PN, Saw SM, Lanca C, et al. Myopia. *Nat Rev Dis Primers*. 2020;6(1):99.

2. Holden B, Sankaridurg P, Smith E, et al. Myopia, an underrated global challenge to vision: where the current data takes us on myopia control. *Eye (Lond)*. 2014;28(2):142–146.
3. Liu C, Li M, Shen Y, et al. Targeting choroidal vasculopathy via up-regulation of tRNA-derived fragment tRF-22 expression for controlling progression of myopia. *J Transl Med*. 2023;21(1):412.
4. Zhou X, Ye C, Wang X, et al. Choroidal blood perfusion as a potential "rapid predictive index" for myopia development and progression. *Eye Vis (Lond)*. 2021;8(1):1.
5. Shi WQ, Li T, Liang R, et al. Targeting scleral remodeling and myopia development in form deprivation myopia through inhibition of EFEMP1 expression. *Biochim Biophys Acta Mol Basis Dis*. 2024;1870(3):166981.
6. Shi WQ, Wan T, Li B, et al. EFEMP1 is a potential biomarker of choroid thickness change in myopia. *Front Neurosci*. 2023;17:1144421.
7. Ogden PJ, Kelsic ED, Sinai S, et al. Comprehensive AAV capsid fitness landscape reveals a viral gene and enables machine-guided design. *Science*. 2019;366(6469):1139–1143.
8. Pietersz KL, Nijhuis PJH, Klunder MHM, et al. Production of high-yield adeno associated vector batches using HEK293 suspension cells. *J Vis Exp*. 2024;206:66532.
9. Wong TF, So PK, Yao ZP. Advances in rapid detection of SARS-CoV-2 by mass spectrometry. *Trends Analyt Chem*. 2022;157:116759.
10. Vitko D, Chou WF, Nouri Golmaei S, et al. timsTOF HT improves protein identification and quantitative reproducibility for deep unbiased plasma protein biomarker discovery. *J Proteome Res*. 2024;23(3):929–938.
11. Boote C, Sigal IA, Grytz R, et al. Scleral structure and biomechanics. *Prog Retin Eye Res*. 2020;74:100773.
12. Liu Y, Wang L, Xu Y, et al. The influence of the choroid on the onset and development of myopia: from perspectives of choroidal thickness and blood flow. *Acta Ophthalmol*. 2021;99(7):730–738.
13. Brown DM, Mazade R, Clarkson-Townsend D, et al. Candidate pathways for retina to scleral signaling in refractive eye growth. *Exp Eye Res*. 2022;219:109071.
14. Wu H, Chen W, Zhao F, et al. Scleral hypoxia is a target for myopia control. *Proc Natl Acad Sci USA*. 2018;115(30):E7091–E7100.
15. Lin X, Lei Y, Pan M, et al. Augmentation of scleral glycolysis promotes myopia through histone lactylation. *Cell Metab*. 2024;36(3):511–525.e517.
16. Roybal CN, Marmorstein LY, Vander Jagt DL, et al. Aberrant accumulation of fibulin-3 in the endoplasmic reticulum leads to activation of the unfolded protein response and VEGF expression. *Invest Ophthalmol Vis Sci*. 2005;46(11):3973–3979.
17. Zhang C, Yu C, Li W, et al. Fibulin-3 affects vascular endothelial function and is regulated by angiotensin II. *Microvasc Res*. 2020;132:104043.
18. Fitzwalter BE, Thorburn A. FOXO3 links autophagy to apoptosis. *Autophagy*. 2018;14(8):1467–1468.
19. Hao W, Dian M, Zhou Y, et al. Autophagy induction promoted by m(6)A reader YTHDF3 through translation upregulation of FOXO3 mRNA. *Nat Commun*. 2022;13(1):5845.
20. Wen Q, Jiao X, Kuang F, et al. FoxO3a inhibiting expression of EPS8 to prevent progression of NSCLC: a new negative loop of EGFR signaling. *EBioMedicine*. 2019;40:198–209.
21. Liu Y, Ao X, Ding W, et al. Critical role of FOXO3a in carcinogenesis. *Mol Cancer*. 2018;17(1):104.
22. Li L, Rispoli R, Patient R, et al. Etv6 activates vegfa expression through positive and negative transcriptional regulatory networks in Xenopus embryos. *Nat Commun*. 2019;10(1):1083.
23. Koenig MN, Naik E, Rohrbeck L, et al. Pro-apoptotic BIM is an essential initiator of physiological endothelial cell death independent of regulation by FOXO3. *Cell Death Differ*. 2014;21(11):1687–1695.
24. Song Y, Zeng S, Zheng G, et al. FOXO3a-driven miRNA signatures suppresses VEGF-A/NRP1 signaling and breast cancer metastasis. *Oncogene*. 2021;40(4):777–790.
25. Zhang J, Ma Y, Zhang Y, et al. Angiogenesis is inhibited by arsenic trioxide through downregulation of the CircHIPK3/miR-149-5p/FOXO1/VEGF Functional Module in Rheumatoid Arthritis. *Front Pharmacol*. 2021;12:751667.
26. Palazon A, Tyrakis PA, Macias D, et al. An HIF-1alpha/VEGF-A axis in cytotoxic T cells regulates tumor progression. *Cancer Cell*. 2017;32(5):669–683.e665.
27. Wang L, Li J, Wang Y, et al. Dan-Deng-Tong-Nao softgel capsule promotes angiogenesis of cerebral microvasculature to protect cerebral ischemia reperfusion injury via activating HIF-1alpha-VEGFA-Notch1 signaling pathway. *Phytomedicine*. 2023;118:154966.
28. Ni H, Li J, Zheng J, et al. Cardamonin attenuates cerebral ischemia/reperfusion injury by activating the HIF-1alpha/VEGFA pathway. *Phytother Res*. 2022;36(4):1736–1747.
29. Huang Y, Liu Z, Li L, et al. Sesamin inhibits hypoxia-stimulated angiogenesis via the NF-kappaB p65/HIF-1alpha/VEGFA signaling pathway in human colorectal cancer. *Food Funct*. 2022;13(17):8989–8997.
30. De Piano M, Cacciamani A, Balzamino BO, et al. Biomarker signature in aqueous humor mirrors lens epithelial cell activation: new biomolecular aspects from cataractogenic myopia. *Biomolecules*. 2023;13(9):1328.
31. Zhou RM, Shi LJ, Shan K, et al. Circular RNA-ZBTB44 regulates the development of choroidal neovascularization. *Theranostics*. 2020;10(7):3293–3307.
32. Mettu PS, Allingham MJ, Cousins SW. Incomplete response to Anti-VEGF therapy in neovascular AMD: exploring disease mechanisms and therapeutic opportunities. *Prog Retin Eye Res*. 2021;82:100906.

Investigative Ophthalmology & Visual Science